KANSAS GEOLOGICAL SURVEY
OPEN-FILE REPORT 89-17

THEORY AND APPLICATION OF AN APPROXIMATE MODEL OF SAT-WATER UPCONING IN AQUIFER

by

Carl McElwee
Marion Kemblowski

Kansas Geological Survey
1930 Constant Avenue
University of Kansas
Lawrence, KS 66047-3726

THEORY AND APPLICATION OF AN APPROXIMATE MODEL OF SALT-WATER UPCONING IN AQUIFERS

Carl McElwee

and

Marian Kemblowski *
Kansas Geological Survey
The University of Kansas
Lawrence, Kansas 66046

Prepared for publication
in
The Journal of Hydrology

Kansas Geological Survey
Open File Report 89-17

*Now at: Shell Development Company, Westhollow Research Center,
P.O. Box 1380, Houston,Texas 77001

ABSTRACT

The motion and mixing of saltwater and freshwater is vitally important for water resource development in many parts of the world. We present the development of an approximate model of saltwater upconing in aquifers, which results in three nonlinear coupled equations for the freshwater zone, the saltwater zone, and the transition zone. This model invokes some reasonable assumptions to give a reasonably tractable model, which is considerably better than the sharp interface approximation, but is considerably simpler than a fully three-dimensional model with variable density. Several numerical techniques can be used to solve the model equations. Some simple analytical solutions can be useful in validating the numerical solution procedures. We find that the model equations can be solved with adequate accuracy using the procedures presented. The approximate model is applied to the Smoky Hill River valley in central Kansas. This model can reproduce earlier sharp interface results; however, it can also evaluate the importance of hydrodynamic dispersion for feeding saltwater to the river. We use a wide range of dispersivity values and find that unstable upconing always occurs. Therefore, in this case, hydrodynamic dispersion is not the only mechanism feeding saltwater to the river. Some simple calculations imply that unstable upconing and hydrodynamic dispersion could be equally important in transporting saltwater to the river. For example, if groundwater flux to the Smoky Hill River were only about 40% of its expected value, a stable upconing situation could exist where hydrodynamic dispersion into a transition zone is the primary mechanism for moving saltwater to the river. It is expected that the current model could be useful in many situations involving dense saltwater layers.

THEORY AND APPLICATION OF AN APPROXIMATE MODEL OF SALT-WATER UPCONING IN AQUIFERS

INTRODUCTION

The motion of the salt-water/fresh-water transition zone due to pumpage in coastal and inland aquifers is of importance for water resources development. Unstable salt-water upwelling or upconing (intrusion of salt water into wells) has caused contamination of many wells. Reilly and Goodman (1985) give a good review of quantitative analysis of salt-water-fresh-water relationships in groundwater systems.

Perhaps the most general description of this problem is given by a variable-density hydrodynamic dispersion model (Bear, 1979); however, the difficulties associated with the numerical solution (mainly due to the numerical dispersion) make this approach impractical in many cases.

One way to avoid these problems is to utilize the sharp interface approximation. This approximation has been used quite extensively by two types of models: 1) a three-dimensional flow model (Liu et al., 1981, Kemblowski, 1984 and 1985), and 2) a horizontal flow model which uses the Dupuit-Forchheimer approximation (Shamir and Dagan, 1971; Mercer et al., 1980; Bear et al., 1985; McElwee, 1985; Essaid, 1986; Kemblowski, 1987). Kemblowski (1987) analyzes the impact of this approximation and concludes that, as long as the size of the sinks or sources (drains, rivers, etc) is of the same order as the thickness of the fresh-water zone, this approximation is quite acceptable. Reilly and Goodman (1987) consider upconing beneath a well and compare the sharp interface results with those of a variable-density hydrodynamic dispersion model. They find that even for stable upconing significant quantities of saltwater will be pumped, and that the development of a transition zone is mainly dependent on the transverse dispersivity.

However, in some cases the sharp interface approach cannot be used. Due to transient boundary conditions (pumpage, river stage fluctuations), a transition zone between the fresh-water and salt-water zones may develop. A simplified description of the transition zone that uses the concept of a boundary layer was presented by Rubin and Pinder (1977) and Rubin (1983). Recent work using the boundary layer approach includes Rubin and Rubin (1986) and Rubin and Pistiner (1986). In this paper, we use this concept to develop a solution for salt-water upconing and to analyze the development of the transition zone. Application to the Smoky Hill River valley in central Kansas is presented.

DEVELOPMENT OF THE MODEL

The development of this solution assumes several approximations; therefore, it is important to emphasize that all of them have to be verified if a practical problem is to be solved. It is assumed that the Dupuit-Forchheimer approximation is valid in the fresh-water and salt-water zones, thus the Darcian velocities in both zones are horizontal. The velocity distribution function (shape function) and the concentration distribution function within the transition zone are also assumed to be known and are similar to finite element basis functions. The velocity distribution is given by

$$\vec{V}_T(\eta) = \vec{U} \cdot F(\eta) + \vec{V} \cdot G(\eta) \tag{1}$$

where $\vec{U}$ and $\vec{V}$ are fresh-water and salt-water Darcian velocities, $\vec{V}_T(\eta)$ is the ground-water velocity in the transition zone, η is a dimensionless vertical coordinate given by

$$\eta = \frac{Z - Z_b}{\delta}. \tag{2}$$

Z is the vertical coordinate, Z_b is the elevation of the bottom of the transition zone, and δ is the transition-zone thickness.

The concentration distribution may be described in a similar manner by

$$C(\eta) = C_F K(\eta) + C_S L(\eta) \tag{3}$$

C_F is the fresh-water concentration and C_S is the salt-water concentration. Assuming that the fresh-water concentration is equal to zero, equation 3 may be simplified to

$$C(\eta) = C_s L(\eta) \tag{4}$$

In the following development, we assume that the aquifer is unconfined. The analysis may be easily modified for confined conditions. Equation 4 may be used to derive a relationship between the fresh-water and salt-water potentials , (ϕ^f and ϕ^s) which are defined by

$$\phi^f = z + p/\gamma_f \tag{5}$$

$$\phi^s = z + p/\gamma_s \tag{6}$$

where p is the pressure and γ_f and γ_s are fresh-water and salt-water specific weights.

Assuming that the flow in the transition zone is horizontal, we obtain the following relationship for the pressure difference between the top and the bottom of the transition zone:

$$\Delta p = p_t - p_b = -\int_{Z_b}^{Z_t} \gamma dZ \tag{7}$$

Z_t is the elevation of the top of the transition zone. Using the following relation between the specific weight and the concentration (the equation of state)

$$\gamma = \gamma_f(1 + \alpha C), \tag{8}$$

we may evaluate the pressure difference as follows:

$$\Delta p = -\int_{Z_b}^{Z_t} \gamma_f(1 + \alpha C)\, dz = -\gamma_f \left(\delta + \alpha C_s\, \delta \int_0^1 L(\eta)\, d\eta \right)$$

$$= -\gamma_f(\delta + \alpha\delta C_s \bar{L}) \tag{9}$$

where $\bar{L} = \int_0^1 L(\eta)\, d\eta$.

This pressure difference may be also estimated from equations 5 and 6.

$$\Delta p = \gamma_f \phi^f - \gamma_s \phi^s - \gamma_f Z_t + \gamma_s Z_b \tag{10}$$

Combining equations 8, 9, and 10 leads to

$$\gamma_f(1 + \alpha C_s)\phi^s - \gamma_f \phi^f + \gamma_f Z_t - \gamma_f(1 + \alpha C_s) Z_b = \gamma_f(\delta + \alpha\delta C_s \bar{L}) \tag{11a}$$

or

$$(1 + \alpha C_s)\phi^s - \phi^f - \alpha C_s Z_b = \alpha\delta C_s \bar{L} \tag{11b}$$

Using equation 11b, the salt-water potential may be expressed as follows:

$$\phi^s = \frac{1}{1+a}\left(\phi^f + aZ_b + a\bar{L}\delta\right) \tag{12}$$

where $a = \alpha C_s$ ·

FLOW CONTINUITY FOR FRESH-WATER AND TRANSITION ZONES

We are considering unconfined ground-water flow in the fresh-water and transition zones. The continuity equation for both zones as a unit may be written as follows:

$$\vec{\nabla} \cdot \left(\vec{q}\right) = -n\frac{\partial \phi^f}{\partial t} + n\frac{\partial Z_b}{\partial t} + N, \tag{13}$$

where:

$\vec{q}$ = horizontal flow rate in the fresh-water and transition zones per unit width $\left(\frac{L^2}{T}\right)$

n = effective porosity (dimensionless)

ϕ^f = fresh-water potential (ground-water level for unconfined conditions) (L)

N = recharge (positive) or discharge (negative) $\left(\frac{L}{T}\right)$

Vector $\vec{q}$ may be expressed by

$$\vec{q} = \vec{U}\left(\phi^f - Z_t\right) + \int_{Z_b}^{Z_t} \vec{V}_T dZ \tag{14}$$

After substituting equation 1 into equation 14, we obtain

$$\vec{q} = \vec{U}\left(\phi^f - Z_t\right) + \delta\,\vec{U}\int_0^1 F(\eta)\,d\eta + \delta\,\vec{V}\int_0^1 G(\eta)\,d\eta\,. \tag{15}$$

When we define $\overline{F}$ and $\overline{G}$ as

$$\overline{F} = \int_0^1 F(\eta)\,d\eta \text{ and } \overline{G} = \int_0^1 G(\eta)\,d\eta, \tag{16}$$

equation 13 may be written as follows:

$$\vec{\nabla}\cdot\left[\left(\phi^f - Z_t + \delta\overline{F}\right)\vec{U} + \delta\overline{G}\,\vec{V}\right] = n\left(\frac{\partial Z_b}{\partial t} - \frac{\partial \phi^f}{\partial t}\right) + N \tag{17}$$

where:

$$\vec{U} = -k_f\,\vec{\nabla}\,\phi^f \tag{18}$$

$$\vec{V} = -k_s\,\vec{\nabla}\,\phi^s\,. \tag{19}$$

k_f and k_s are hydraulic conductivities in the fresh-and salt-water zones, respectively.

Substituting equations 12, 18, and 19 into equation 17, we obtain

$$\vec{\nabla}\cdot\left[k_f\left(\phi^f - Z_t + \delta\overline{F}\right)\vec{\nabla}\,\phi^f + \frac{k_s\delta\overline{G}}{1+a}\left(\vec{\nabla}\,\phi^f + a\,\vec{\nabla}\,Z_b + a\overline{L}\,\vec{\nabla}\,\delta\right)\right]$$

$$= n\left(\frac{\partial\phi^f}{\partial t} - \frac{\partial Z_b}{\partial t}\right) - N. \tag{20}$$

Defining

$$A_1 = k_f\left(\phi^f - Z_t + \delta\overline{F}\right) + \frac{k_s\delta\overline{G}}{1+a}, \tag{21}$$

$$B_1 = \frac{k_s \delta \overline{G} a}{1 + a} \tag{22a}$$

and

$$C_1 = B_1 \overline{L} \tag{22b}$$

equation 20 may be written as follows:

$$\vec{\nabla} \cdot \left(A_1 \vec{\nabla} \phi^f + B_1 \vec{\nabla} Z_b + C_1 \vec{\nabla} \delta \right) = n \left(\frac{\partial \phi^f}{\partial t} - \frac{\partial Z_b}{\partial t} \right) - N. \tag{23}$$

MASS TRANSPORT IN THE TRANSITION ZONE

The solute transport in the transition zone is assumed to be of the advection type, with the exception of dispersive salt-water flux at the bottom of the transition zone. Under such assumptions the horizontal mass transport equation may be written as follows:

$$\vec{\nabla} \cdot \vec{Q} = -\frac{\partial M}{\partial t} - nD_T \frac{\partial C}{\partial Z}\bigg|_{Z_b} + P \tag{24}$$

where

$\vec{Q}$ = solute mass flux in the transition zone,
M = mass of the solute in the transition zone,
D_T = transverse dispersion coefficient at the bottom of the transition zone and
P = a source or sink in the transition zone.

The transverse dispersion coefficient is further defined as

$$D_T = \frac{\alpha_T}{n} \left| \vec{U} \right| + D_f \tag{25}$$

α_T is the tranverse dispersivity and D_f is the molecular diffusion constant.

The solute mass flux in equation 24 may be calculated as follows:

$$\vec{Q} = \int_{Z_b}^{Z_t} \vec{V}_T \, C dz = C_s \delta \left[\vec{U} \int_0^1 F(\eta) L(\eta) d\eta + \vec{V} \int_0^1 G(\eta) L(\eta) d\eta \right] . \tag{26}$$

Denoting

$$\overline{FL} = \int_0^1 F(\eta) L(\eta) \, d\eta, \text{ and } \overline{GL} = \int_0^1 G(\eta) L(\eta) \, d\eta, \tag{27}$$

we obtain

$$\vec{Q} = C_s \left(\delta \, \vec{U} \, \overline{FL} \right) + \delta \, \vec{V} \, \overline{GL} \tag{28}$$

The second term in equation 24 may be expressed as follows:

$$\frac{\partial M}{\partial t} = \frac{\partial}{\partial t} \left(\int_{Z_b}^{Z_t} nCdz \right) = \frac{\partial}{\partial t} \left(\delta n C_s \int_0^1 L(\eta) \, d\eta \right)$$

$$= nC_s \overline{L} \, \frac{\partial \delta}{\partial t} \tag{29}$$

The dispersive flow through the bottom of the transition zone may be written as

$$nD_T \left. \frac{\partial C}{\partial Z} \right|_{Z_b} = nD_T \left[\frac{\partial C}{\partial \eta} \, \frac{\partial \eta}{\partial Z} \right]_{\eta=0} = \frac{nD_T C_s}{\delta} \left. \frac{dL(\eta)}{d\eta} \right|_{\eta=0} \tag{30}$$

Denoting

$$L'(0) = \left. \frac{dL(\eta)}{d\eta} \right|_{\eta=0}, \tag{31}$$

we obtain

$$nD_T \frac{\partial C}{\partial Z}\bigg|_{Z_b} = n\, D_T C_s L'(0)/\delta. \tag{32}$$

In equation 24, P represents the solute mass flux due to a source or sink that is operative in the transition zone. Suppose Q_p is the strength of the source or sink that is evenly distributed vertically through the fresh and transition zones considered as a single unit. We will only consider a sink for P. In that case, the water pumped will have the appropriate concentration for the transition zone. The total solute mass flux is obtained by integrating over the transition zone.

$$P = \frac{Q_p}{\left(\phi^f - Z_b\right)} \int_{Z_b}^{Z_t} C dZ = \frac{Q_p \delta C_s}{\left(\phi^f - Z_b\right)} \int_0^1 L(\eta)\, d\eta$$

$$P = \frac{C_s Q_p \delta \overline{L}}{\left(\phi^f - Z_b\right)}\,. \tag{33}$$

Substituting equations 28, 29, 32, 33, 18, 19, and 12 into equation 24 we obtain

$$\vec{\nabla} \cdot \left[\delta\left(k_f \overline{FL} + \frac{k_s \overline{GL}}{1+a}\right) \vec{\nabla}\phi^f + \delta \frac{k_s \overline{GLa}}{1+a} \vec{\nabla} Z_b + \delta \frac{k_s \overline{GLa\overline{L}}}{1+a} \vec{\nabla}\delta\right]$$

$$= n\overline{L}\frac{\partial \delta}{\partial t} + nD_T L'(0)/\delta - \frac{Q_p \delta \overline{L}}{\left(\phi^f - Z_b\right)} \tag{34}$$

Equation 34 can be simplified by defining

$$A_2 = \left(k_f \overline{FL} + \frac{k_s \overline{GL}}{1 + a} \right) \tag{35}$$

$$B_2 = \left(\frac{k_s \overline{GL}\, a}{1 + a} \right) \tag{36}$$

$$C_2 = B_2 \overline{L} \tag{37}$$

The resulting form for equation 34 is

$$\vec{\nabla} \cdot \left(A_2 \delta \, \vec{\nabla} \phi^f + B_2 \delta \, \vec{\nabla} Z_b + C_2 \delta \, \vec{\nabla} \delta \right) = n\overline{L} \frac{\partial \delta}{\partial t} + nD_T L'(0)/\delta - \frac{Q_p \delta \overline{L}}{\left(\phi^f - Z_b \right)} \tag{38}$$

which is very similar to equation 23.

FLOW CONTINUITY IN THE SALT-WATER ZONE

Salt-water flow continuity may be written as follows:

$$\vec{\nabla} \cdot \left(\vec{q}_s \right) = -\, n \frac{\partial Z_b}{\partial t} + Q_s \tag{39}$$

where

$$\vec{q}_s = (Z_b - Z_B)\, \vec{V} \tag{40}$$

Z_B	=	the elevation of the bottom of the aquifer.
Q_s	=	areal"recharge" of salt water in the salt-water zone from underlying formations), may be expressed as a function of the salt-water potential (leaky acquifer conditions).

Substituting equations 12, 19, and 40 into equation 39, we obtain

$$\vec{\nabla} \cdot \left[k_s(Z_b - Z_B)/(1 + a) \left(\vec{\nabla} \phi^f + a \vec{\nabla} Z_b + a\bar{L} \vec{\nabla} \delta \right) \right]$$

$$= n \frac{\partial Z_b}{\partial t} - Q_s \tag{41}$$

Introducing the coefficients

$$A_3 = \frac{k_s(Z_b - Z_B)}{1 + a} \tag{42}$$

$$B_3 = A_3 a \tag{43}$$

$$C_3 = B_3 \bar{L} \tag{44}$$

allows equation 41 to be written as

$$\vec{\nabla} \cdot \left(A_3 \vec{\nabla} \phi^f + B_3 \vec{\nabla} Z_b + C_3 \vec{\nabla} \delta \right) = n \frac{\partial Z_b}{\partial t} - Q_s \cdot \tag{45}$$

Equations 23, 38, and 45 complete the mathematical description of the approximate model of salt-water upconing.

SHAPE FUNCTIONS OF VELOCITY AND CONCENTRATION

The velocity distribution within the transition zone is approximated by equation 1. The boundary conditions, which shape functions $F(\eta)$ and $G(\eta)$ are to satisfy, are

$$F(0) = 0 \qquad F(1) = 1 \tag{46}$$

$$\frac{dF}{d\eta}(0) = 0 \qquad \frac{dF}{d\eta}(1) = 0 \tag{47}$$

$$G(0) = 1 \qquad G(1) = 0 \tag{48}$$

$$\frac{dG}{d\eta}(0) = 0 \qquad \frac{dG}{d\eta}(1) = 0. \tag{49}$$

The conditions given by equations 47 and 49 are not necessary; however, they assure the smoothness of the velocity distribution.

The lowest order polynomials that satisfy equations 46 through 49 are given by

$$F(\eta) = -2\eta^3 + 3\eta^2 \tag{50}$$

$$G(\eta) = 2\eta^3 - 3\eta^2 + 1. \tag{51}$$

The values of the integrals in equation 16 may now be calculated:

$$\overline{F} = \int_0^1 (-2\eta^3 + 3\eta^2) = 1/2 \tag{52}$$

$$\overline{G}(\eta) = \int_0^1 (2\eta^3 - 3\eta^2 + 1)\, d\eta = 1/2 \tag{53}$$

The shape function of the concentration distribution ($L(\eta)$ in equation 4) has the following boundary conditions:

$$L(0) = 1 \qquad\qquad L(1) = 0 \tag{54}$$

$$\frac{dL}{d\eta}(1) = 0 \cdot \tag{55}$$

The lowest order polynomial that satisfies this equation is given by

$$L(\eta) = \eta^2 - 2\eta + 1 \tag{56}$$

The derivative of this function at the bottom of the transition zone (which is related to the concentration gradient and therefore to the dispersion through the bottom of the transition zone, given by equation 32) can now be evaluated.

$$L'(0) = \left.\frac{dL(\eta)}{d\eta}\right|_{\eta=0} = -2 \tag{57}$$

The values of the integrals in equations 9 and 27 may now be calculated

$$\overline{L} = \int_0^1 (\eta^2 - 2\eta + 1)\, d\eta = 1/3 \tag{58}$$

$$\overline{FL} = \int_0^1 F(\eta)L(\eta)\, d\eta = 1/15 \tag{59}$$

$$\overline{GL} = \int_0^1 L(\eta)G(\eta)\, d\eta = 4/15 \tag{60}$$

Rubin and Pistiner (1986) present an extensive discussion of shape functions.

TRANSFORMATION OF TRANSITION ZONE EQUATION

Equation 38, which describes solute transport in the transition zone, can be transformed to a more suitable form for solution. In its present form there appears to be a problem as δ approaches zero. Actually, when $\delta = 0$ this equation is no longer needed and we have the sharp interface description with only two equations, 23 and 45. However, some insight is gained into the nature of the equation by the following transformation. Multiplying through by δ and remembering that

$$\delta \vec{\nabla} \delta = \frac{1}{2} \vec{\nabla} \delta^2$$

and

$$\delta \frac{\partial \delta}{\partial t} = \frac{1}{2} \frac{\partial \delta^2}{\partial t}$$

gives

$$\delta \vec{\nabla} \cdot \left(C_2 \vec{\nabla} \delta^2 \right) + \left[A_2 \vec{\nabla} \phi^f + B_2 \vec{\nabla} Z_b \right] \cdot \vec{\nabla} \delta^2 + 2\left[A_2 \nabla^2 \phi^f + B_2 \nabla^2 Z_b \right] \delta^2$$

$$= n\bar{L} \frac{\partial \delta^2}{\partial t} + 2nD_T L'(0) - \frac{2Q_p \bar{L}}{\left(\phi^f - Z_b \right)} \delta^2 \qquad (61)$$

If it were not for the first term in this equation, it would be clearly hyperbolic in δ^2. The terms involving undifferentiated δ^2 represent loss or gain of solute from the transition zone. The constant term involving D_T is responsible for widening the transition zone by hydrodynamic dispersion. The first term has the usual form of a diffusive or parabolic equation except for the factor of δ which makes it nonlinear. This first term is usually a secondary effect which simply makes the solution smoother than the purely hyperbolic solution. However, there will always be some numerical dispersion, which also introduces smoothing, in a finite difference solution to equation 61. It has been our experience, for problems considered in this paper, that the numerical dispersion and the first term of equation 61 are of comparable magnitude, neither of which are dominant effects.

NUMERICAL SOLUTION

Equations 23, 45, and 61 form a set of three simultaneous equations which must be solved for ϕ^f, Z_b, and δ. For a complete solution appropriate boundary conditions and initial conditions must also be given. The left-hand side of all three equations contains terms of the following form:

$$\frac{\partial}{\partial x}\left(W\frac{\partial U}{\partial x}\right) \tag{62}$$

In order to implement a numerical solution, a grid system with grid spacing Δx is introduced in the x direction. Since the three equations are vertically averaged and since we are only considering a cross-sectional model, no spatial derivatives other than x appear in $\vec{\nabla}$.

A centered finite difference approximation to equation 62, located at node i, is given by

$$\left[\frac{\partial}{\partial x}\left(W\frac{\partial U}{\partial x}\right)\right]_i = \Big[W_{i+\frac{1}{2}}\,U_{i+1} - \left(W_{i+\frac{1}{2}} + W_{i-\frac{1}{2}}\right)U_i + W_{i-\frac{1}{2}}U_{i-1}\Big]/\Delta x^2 \tag{63}$$

The half-integer values of W are usually evaluated at node points by the approximation

$$W_{i+\frac{1}{2}} = \frac{1}{2}(W_{i+1} + W_i) \tag{64}$$

Using this approximation, equation 63 becomes

$$\left[\frac{\partial}{\partial x}\left(W\frac{\partial U}{\partial x}\right)\right]_i = \left[(W_{i+1} + W_i)\,U_{i+1} - (W_{i+1} + 2W_i + W_{i-1})U_i + (W_i + W_{i-1})U_{i-1}\right]/2\Delta x^2 \tag{65}$$

In equation 65, as applied to equations 23, 45, and 61 or 38, W may be $A_1, A_2, A_3, B_1, B_2, B_3, C_1, C_2,$ or C_3 and U may be $\phi^f, Z_b,$ or δ^2.

Equation 61 also requires numerical approximations for $\vec{\nabla}\, U$ and $\nabla^2 U$. The usual centered difference formulas are used

$$\frac{\partial U}{\partial x} = \frac{U_{i+1} - U_{i-1}}{2\Delta x} \tag{66a}$$

or

$$\frac{\partial U}{\partial x} = \frac{U_{i+\frac{1}{2}} - U_{i-\frac{1}{2}}}{\Delta x} \tag{66b}$$

and

$$\frac{\partial^2 U}{\partial x^2} = \frac{U_{i+1} - 2U_i + U_{i-1}}{\Delta x^2} \tag{67}$$

where U may be ϕ^f, Z_b, or δ^2.

In addition to spatial derivatives, the right-hand sides of equations 23, 45, and 61 or 38 involve various time derivatives. These time derivatives may be approximated several ways. We consider the usual three ways. Let time be discretized into intervals Δt and let m, when used as a superscript, denote the m th time step. If m is the current time step for which values are known (either from the initial conditions or a previous time step solution) then m+1 represents the unknown values at a new time step which are to be solved for. The time derivative may be evaluated as

$$\left[\frac{\partial U}{\partial t}\right]_i^m = \frac{U_i^{m+1} - U_i^m}{\Delta t} \tag{68a}$$

$$\left[\frac{\partial U}{\partial t}\right]_i^{m+1} = \frac{U_i^{m+1} - U_i^m}{\Delta t} \tag{68b}$$

or

$$\left[\frac{\partial U}{\partial t}\right]_i^{m+\frac{1}{2}} = \frac{U_i^{m+1} - U_i^m}{\Delta t} \tag{68c}$$

Equation 68a implies the whole equation is evaluated at time m, and the end result is an explicit procedure with its attendant restriction on time step magnitude. Equation 68b indicates the entire difference equation is evaluated at time m+1 and gives an implicit procedure. The usual Crank-Nicolson procedure is indicated by equation 68C, where the difference equation is evaluated at time $m + \frac{1}{2}$ by using the usual approximation

$$U_i^{m+\frac{1}{2}} = \frac{1}{2}\left[U_i^{m+1} + U_i^m\right]. \tag{69}$$

In equations 66 through 69 U may be ϕ^f, Z_b, or δ^2.

The explicit procedure gives the simplest equations to work with since the new time level values are generated individually from the old time values with no need to solve simultaneous equations. Since equation 23 involves both ϕ^f and Z_b at the new time level, it should be solved last or at least after equation 45 has been solved for Z_b at the new time level. However, rather stringent time step restrictions are required to keep the solution stable with increasing time. This time step restriction may make it difficult to reach steady state in some situations. As an example, consider equation 61 in explicit form ready to be solved for the new time step value. For convenience we let $y = \delta^2$.

$$y_i^{m+1} = y_i^m\left[1 + E_i^m\right]\Delta t - \left[\frac{2D_T L'(0)}{\bar{L}}\right]_i^m \Delta t + \vec{F}^m{}_i \Delta t \cdot \left[\vec{\nabla} y\right]_i^m$$

$$+ \left[\frac{C_2}{n\bar{L}} y^{\frac{1}{2}}\right]_i^m \Delta t\left[\nabla^2 y\right]_i^m \tag{70}$$

E_i^m and $\vec{F}_i^m$ are defined as follows.

$$E_i^m = \left[2\left(A_2 \nabla^2 \phi^f + B_2 \nabla^2 Z_b\right)/n\bar{L} + 2Q_p/n\left(\phi^f - Z_b\right)\right]_i^m \tag{71}$$

$$\vec{F}_i^m = \left[\left(A_2\, \vec{\nabla}\, \phi^f + B_2\, \vec{\nabla}\, Z_b\right)/n\, \vec{L}\right]_i^m \tag{72}$$

It is well known (Press et al., 1985) that if E_i^m and C_2 in equation 70 are zero, equation (70) is unstable for any Δt. This problem can be cured by using the Lax method which consists of replacing y_i^m by ($y_{i+1}^m + y_{i-1}^m$)/2. However, for small time steps the Lax method introduces considerable numerical dispersion. We have introduced a more general weighing for y_i^m given by

$$y_i^m \rightarrow \tfrac{1}{2}(y_{i+1}^m + y_{i-1}^m)(1 - \varepsilon) + y_i^m \varepsilon \tag{73}$$

When $\varepsilon = 0$ we have the Lax method, while $\varepsilon = 1$ gives equation 70 again. We found this useful because when equation 70 can be used it gives less numerical dispersion than the Lax method.

With the new weighting scheme of equation 73, equation 70 takes the form

$$y_i^m = \left[\tfrac{1}{2}(y_{i+1}^m + y_{i-1}^m)\,(1-\varepsilon) + y_i^m\varepsilon\right]\left[1 + E_i^m\right]\Delta t - \left[\frac{2D_T L'(0)}{\overline{L}}\right]_i^m \Delta t$$

$$+ \vec{F}_i^m\,\Delta t \cdot \left[\vec{\nabla} y\right]_i^m + \left[\frac{C_2}{n\overline{L}}\,y^{\frac{1}{2}}\right]_i^m \Delta t\left[\nabla^2 y\right]_i^m \qquad (74)$$

We have performed a von Neuman stability analysis (Press et al., 1985) on equation 74, which is strictly valid only for the case where E_i^m, $\vec{F}_i^m$, D_T, and $C_2 y^{\frac{1}{2}}$ are constants. However, we assume their variation is slow so the analysis can be done because we need some guidance in choosing the time step. The results are summarized in the next three equations.

$$\Delta t \le \sqrt{1-\varepsilon^2}\;\frac{\Delta x}{\left|\vec{F}_i^m\right|} \quad \text{for all i,m} \qquad (75)$$

$$\Delta t \le 2/\left|E_i^m\right| \quad \text{for all i,m} \qquad (76)$$

$$\Delta t \le \varepsilon\Delta x^2\left[n\overline{L}/2\delta C_2\right]_i^m \quad \text{for all i,m} \qquad (77)$$

We have found for the work of this paper that $\varepsilon = .9$ is a good choice; it doesn't cause too much numerical dispersion and it is stable given suitable restrictions on the time step such as equations 75 through 77. Equations 75-77 do not guarantee stability for highly nonlinear problems with strong coupling between the three zones (freshwater layer, transition layer, and saltwater layer); however, we have found them to be adequate for this work. In any case, one can always choose a smaller Δt if instability occurs.

Explicit formulations for equations 23 and 45 can be determined in a similar way. However, they seem to be primarily parabolic so we do not need to consider the Lax method or a general weighting scheme for them. A stability analysis for these two equations under the same assumptions as before yields

$$\Delta t \leq n\Delta x^2/2[A_1]_i^m \text{ for all } i,m \tag{78}$$

for the freshwater layer (equation 23) and

$$\Delta t \leq n\Delta x^2/2[B_3]_i^m \text{ for all } i,m \tag{79}$$

for the saltwater layer (equation 45).

If an implicit or Crank-Nicolson formulation is used for equations 23, 45, and 61, the equations are more difficult to solve. However, stability problems are not expected, except in the most strongly nonlinear cases. This means that the time step can be accelerated as we approach steady state. This is a nice feature since it is sometimes difficult to reach steady state efficiently with an explicit formulation which has time step restrictions such as equations 75 through 79.

Using an implicit procedure (equation 68b) on equation 23 gives

$$\left(\frac{A_{1i+1}+A_{1i}}{2\Delta x^2}\right)^{m+1}\phi^{f\,m+1}_{i+1}-\left(\frac{A_{1i+1}+2A_{1i}+A_{1i-1}}{2\Delta x^2}+\frac{n}{\Delta t}\right)^{m+1}\phi^{f\,m+1}_{i}$$

$$+\left(\frac{A_{1i}+A_{1i-1}}{2\Delta x^2}\right)^{m+1}\phi^{f\,m+1}_{i-1}+\left(\frac{B_{1i+1}+B_{1i}}{2\Delta x^2}\right)^{m+1}Z^{m+1}_{b\,i+1}$$

$$+\left(\frac{n}{\Delta t}-\frac{B_{1i+1}+2B_{1i}+B_{1i-1}}{2\Delta x^2}\right)^{m+1}Z^{m+1}_{bi}+\left(\frac{B_{1i}+B_{1i-1}}{2\Delta x^2}\right)^{m+1}Z^{m+1}_{b\,i-1}$$

$$+\left(\frac{C_{1i+1}+C_{1i}}{2\Delta x^2}\right)^{m+1}\delta^{m+1}_{i+1}-\left(\frac{C_{1i+1}+2C_{1i}+C_{1i-1}}{2\Delta x^2}\right)^{m+1}\delta^{m+1}_{i}$$

$$+\left(\frac{C_{1i}+C_{1i-1}}{2\Delta x^2}\right)^{m+1}\delta^{m+1}_{i-1}=\frac{n}{\Delta t}\left(Z^{m}_{bi}-\phi^{f\,m}_{i}\right)-N^{m+1}_{i}\,. \tag{80}$$

In equation 80 the new time level values of the dependent variables have been collected on the left, while the known previous time level values and the recharge (which should be known) have been kept on the righthand side. If we consider A, B, and C known, then equation 80 has nine unknowns and can be written for each active node.

Equations similar to 80 can be written for equation 38 or 61 and equation 45. These equations form a tri-tridiagonal system of equations. Von Rosenberg (1969) has shown how to solve such a set of simultaneous equations directly. He gives an efficient algorithm which takes advantage of the sparseness of the coefficient matrix. If we have N active nodes, it is seen that the implicit equations form a 3N x 3N set of matrix equations to be solved for the 3N unknowns. ϕ^f, Z_b and δ must be found for each of the N active nodes. However, it is clear from equation 80 that only a maximum of 9 unknowns appear in each equation. Therefore, in the 3N x 3N matrix, only a central band of 9 diagonals is nonzero. In fact, the three implicit equations only have 6 unknowns for the first and last active nodes. This is so because some type of boundary condition must be applied at the ends of the model and this eliminates 3 of the unknowns. We have written a program to implement von Rosenberg's tri-tridiagonal solution (Kemblowski and McElwee, 1986).

Unfortunately, a single solution of the implicit equations for a given time step does not give the correct answer, since the coefficients in the implicit equations (equation 80 is an example) are themselves functions of ϕ^f, Z_b and δ at the new time level m + 1. In other words, we have a nonlinear set of equations. Therefore, an iterative scheme must be used at each time step until sufficient accuracy has been obtained. At the beginning of each time step the preceding time step values of ϕ^f, Z_b and δ may be used to evaluate the coefficients and start a new iteration. Alternately some projection scheme can be used to start each new time step. Iteration ceases when there is little change between iterations in ϕ^f, Z_b and δ. This convergence criteria is specified for the problem under consideration.

The use of a point iterative technique alleviates the need to solve a system of simultaneous equations as outlined previously for the implicit method. As an example, consider equation 45 for the saltwater zone written in the Crank-Nicolson form using equations 68c and 69.

$$\left[\vec{\nabla}\cdot\left(A_3\vec{\nabla}\phi^f + C_3\nabla\delta\right)\right]_i^{m+\frac{1}{2}} + \frac{1}{2}\left[\vec{\nabla}\cdot\left(B_3\vec{\nabla}Z_b\right)\right]_i^{m+1} + \frac{1}{2}\left[\vec{\nabla}\cdot\left(B_3\vec{\nabla}Z_b\right)\right]_i^{m}$$

$$= n\left(\frac{Z_{bi}^{m+1} - Z_{bi}^{m}}{\Delta t}\right) - Q_{si}^{m+\frac{1}{2}} \qquad (81)$$

Applying equation 66b twice allows us to write

$$\left[\vec{\nabla} \cdot \left(B_3 \vec{\nabla} Z_b\right)\right]_i^{m+1} = \left[\frac{B_3}{\Delta x^2}\right]_{i+\frac{1}{2}}^{m+1} Z_{b\,i+1}^{m+1} - \left\{\left[\frac{B_3}{\Delta x^2}\right]_{i+\frac{1}{2}}^{m+1} + \left[\frac{B_3}{\Delta x^2}\right]_{i-\frac{1}{2}}^{m+1}\right\} Z_{bi}^{m+1}$$

$$+ \left[\frac{B_3}{\Delta x^2}\right]_{i-\frac{1}{2}}^{m+1} Z_{b\,i-1}^{m+1} \qquad (82)$$

When equation 82 is used in equation 81 the resulting equation can be solved for Z_{bi}^{m+1} to give

$$Z_{bi}^{m+1} = \left\{\left[\vec{\nabla} \cdot \left(A_3 \vec{\nabla}^f + C_3 \vec{\nabla}\right)\right]_i^{m+\frac{1}{2}} + \frac{1}{2}\left[\vec{\nabla} \cdot \left(B_3 \vec{\nabla} Z_b\right)\right]_i^m\right.$$

$$\left. + \frac{1}{2}\left[\frac{B_3}{\Delta x^2}\right]_{i+\frac{1}{2}}^{m+1} Z_{b\,i+1}^{m+1} + \frac{1}{2}\left[\frac{B_3}{\Delta x^2}\right]_{i-\frac{1}{2}}^{m+1} Z_{b\,i-1}^{m+1} + \frac{n}{\Delta t} Z_{bi}^m + Q_{si}^{m+\frac{1}{2}}\right\}$$

$$\cdot \left\{\frac{n}{\Delta t} + \left[\frac{B_3}{\Delta x^2}\right]_{i+\frac{1}{2}}^{m+1} + \left[\frac{B_3}{\Delta x^2}\right]_{i-\frac{1}{2}}^{m+1}\right\}^{-1} \qquad (83)$$

Equation 83 contains unknowns of ϕ^f, Z_b and δ at the new time level on the right side. Therefore, an iterative scheme must be used until there is negligible change in the unknown variables between two iterations. If the new iteration values of ϕ^f, Z_b and δ at the new time level are used in equation 83 as soon as they are obtained, the technique is called Gauss-Seidel iteration (von Rosenberg, 1969). This method does not involve solving simultaneous algebraic equations; however, one might suppose several iterations would be required since we are iterating for two reasons. As in the implicit method discussed earlier, the equations are nonlinear and will always require iterations to solve them. Secondly, we have effectively decoupled the simultaneous equations between iterations. Since we have to iterate due to the nonlinearity anyway, it seems that this might be the most logical way to proceed. It is certainly easier to program than a simultaneous solution algorithm. However, except in the most nonlinear cases there should be no stability problems associated with the time step. The old time step values can be used to start an iteration, or some projection scheme can be used to start with an improved value.

We have used all of the above described methods in solving equations 23, 45 and 38 or 61. Mainly, so results could be cross checked between programs. However, each technique has its strong points and weak points. The explicit method is easy to program but difficult to run to steady state sometimes. The implicit method described here is perhaps the most robust with regard to time step stability but it is difficult to program. The Crank-Nicolson point iterative technique is perhaps a good compromise between the other two. It is easy to program and has no time step stability restrictions.

ANALYTICAL SOLUTIONS

In the previous section we discussed several ways of numerically solving equations 23, 45 and 38 or 61. Any numerical technique is an approximation to the real solution. Also, it is easy to make mistakes when programming a numerical technique. For these reasons, it is a great advantage to have some analytical solutions to which one can compare the numerical results. Unfortunately, there are not many analytical solutions available; and, they are for relatively simple situations. We present a couple of solutions that have been helpful in this work.

We shall consider the transition zone first. Kemblowski and Colthart (1989) have presented some analytical solutions for a transition zone between a hydrocarbon-groundwater interface. We follow a parallel development here. If we assume $\nabla^2\phi^f = 0$, $\nabla^2 Z_b = 0$, and $C_2 = 0$ and use $y = \delta^2$ equation 61 becomes

$$\left[A_2\,\vec{\nabla}\phi^f + B_2\,\vec{\nabla}Z_b\right]\cdot\vec{\nabla}y = n\bar{L}\frac{\partial y}{\partial t} + 2n\,D_T L'(0) - \frac{2Q_p\bar{L}y}{\left(Q^f - Z_b\right)} \qquad (84)$$

In general, equation 84 still cannot be solved analytically. However, with some additional assumptions two analytical solutions can be obtained. First consider the case where $\vec{\nabla}\phi^f = \vec{\nabla}Z_b = G = \text{constant}$. This condition means that ϕ^f and Z_b are parallel and maintain the same thickness which we call T. With these assumptions equation 84 becomes

$$[A_2 + B_2]G\frac{\partial y}{\partial x} = n\bar{L}\frac{\partial y}{\partial t} + 2n\,D_T L'(0) - \frac{2Q_p\bar{L}}{T}y \qquad (85)$$

The quantity

$$v_h = -\,[A_2 + B_2]G/n\bar{L} \qquad (86)$$

plays the role of a propagation velocity in equation 85 which is now clearly hyperbolic. The steady state solution to equation 85 is

$$\delta^2 = y = \frac{nD_T L'(0)T}{Q_p\bar{L}} + \beta\,\mathrm{EXP}\left[-\frac{2Q_p\bar{L}x}{T(A_2 + B_2)G}\right] \qquad (87)$$

where

$$\beta = y(0) - \frac{nD_T L'(0)T}{Q_p \bar{L}} \tag{88}$$

and y(0) is the boundary value of δ^2 at x = 0. The method of characteristics (Williams, 1980) allows the transient solution of 85 to be written as

$$\delta^2 = \begin{cases} \dfrac{nD_T L'(0)T}{Q_p \bar{L}} + \beta \, \mathrm{EXP}\left[\dfrac{2Q_p t}{nT}\right] & x > v_h t \\[2ex] \dfrac{nD_T L'(0)T}{Q_p \bar{L}} + \beta \, \mathrm{EXP}\left[-\dfrac{2Q_p \bar{L} x}{T(A_2 + B_2)G}\right] & x \le v_h t \end{cases} \tag{89}$$

A slight variation will produce another analytical solution to equation 84. If there is no pumpage from the transition zone $(Q_p = 0)$, then it does not matter if ϕ^f and Z_b are not parallel. However, we still assume that ϕ^f and Z_b are straight lines; i.e., $\nabla \phi^f = G_1$ and $\nabla Z_b = G_2$. With these assumptions equation (84) becomes

$$[A_2 G_1 + B_2 G_2] \frac{\partial y}{\partial x} + n\bar{L} \frac{\partial y}{\partial t} + 2n \, D_T \, L'(0), \qquad (90$$

where

$$v_h = -\left[\frac{A_2 G_1 + B_2 G_2}{n\bar{L}}\right] \tag{91}$$

is now the hyperbolic propagation velocity. The steady state solution to equation (90) is

$$\delta^2 = y = y(0) + \frac{2n \, D_T L'(0) x}{[A_2 G_1 + B_2 G_2]} \qquad (92$$

Again the method of characteristics can be used to obtain the transient solution.

$$\delta^2 = \begin{cases} \delta^2(0) - \dfrac{2n\, D_T L'(0) t}{n\, \bar{L}} & x > v_h t \\ \\ \delta^2(0) + \dfrac{2n\, D_T L'(0) x}{[A_2 G_1 + B_2 G_2]} & x \le v_h t \end{cases} \tag{93}$$

An analytical solution for ϕ^f and Z_b would be useful, since previous analytical solutions presented here dealt only with δ for a given ϕ^f and Z_b .There are a number of well known simple analytical solutions for ϕ^f only, when $\delta = 0$ and $Z_b = 0$. These are useful for checking the ϕ^f part of the program. However, a simultaneous solution for ϕ^f and Z_b would be most useful. If we choose $\delta = 0$ we have the sharp interface approximation. Unfortunately, even analytical solutions to the sharp interface approximation are available only for the simplest cases. Bear et al. (1985) and Bear and Verruijt (1987) present a steady state solution for a coastal aquifer. We follow a similar development to obtain an analytical solution that is useful for this paper.

For steady state and the sharp interface approximation ($\delta = 0$), equation 23 becomes

$$\vec{\nabla}\left[K_f\left(\phi^f Z_b\right) \vec{\nabla}\, \phi^f\right] = -N \tag{94}$$

However, this equation cannot be solved by itself since it is coupled to Z_b. Normally, equation 94 must be solved simultaneously with the steady-state sharp-interface version of equation 45. However, if we assume that no saltwater flows at steady state then ϕ^s must be a constant; and consequently, $\vec{\nabla}\phi^s$ must be zero. From equation 12

$$\vec{\nabla}\phi^s = \frac{1}{1+a}\left(\vec{\nabla}\phi^f + a\,\vec{\nabla}Z_b\right) = 0 \tag{95}$$

$$\phi^s = \frac{1}{1+a}\left(\phi^f + a\,Z_b\right) = \text{constant} \tag{96}$$

For the cross-sectional models used in this paper ϕ^s, ϕ^f, and Z_b are functions of only one space variable x. Assume that boundary values of ϕ^f and Z_b are given at $x = 0$ as $\phi^f(0)$ and $Z_b(0)$. The resulting constant saltwater potential is

$$\phi^s = \frac{1}{1+a}\left(\phi^f(0) + a\,Z_b(0)\right) \tag{97}$$

With a little algebraic manipulation, and using equation 96 to eliminate Z_b, equation 94 yields

$$\nabla^2\left(\phi^f - \phi^s\right)^2 = -\frac{2aN}{(1+a)K_f} \tag{98}$$

for a homogeneous hydraulic conductivity. It is easy to show that the general solution to equation 98 is

$$\left[\phi^f(x) - \phi^s\right]^2 = -\frac{aNx^2}{(1+a)K_f} + 2\left[\phi^f(0) - \phi^s\right]\left[\frac{\partial\phi^f}{\partial x}\right]_{x=0}\cdot x$$

$$+\left[\frac{a}{1+a}\right]^2\left[\phi^f(0) - Z_b(0)\right]^2 \tag{99}$$

where $\left[\frac{\partial \phi^f}{\partial x}\right]_{x=0}$, $\phi^f(0)$, and $Z_b(0)$ are the boundary conditions at x = 0. ϕ^s is a constant given by equation 97. The value of Z_b is found from equation 96 using the solution ϕ^f from equation 99.

$$Z_b(x) = \left[\frac{1+a}{a}\right]\phi^s - \frac{1}{a}\phi^f(x) \qquad (100)$$

Equations 99, 100, and 97 give a complete analytical solution for ϕ^f and Z_b at steady state when there is no saltwater flow and the hydraulic conductivity is homogeneous.

AREA OF APPLICATION

The area of application for this study is the alluvial river valley of the Smoky Hill River between Salina and Solomon in Central Kansas. McElwee (1985) has worked with this area using the sharp interface approximation. In applying the transition zone model presented in this paper, we will use the same physical parameters he used. These are only gross averages for the area and cannot be considered site specific.

$$\begin{aligned}
k_f &= 300 \text{ ft/day} \\
n &= .15 \\
N &= .00197 \text{ ft/day} \\
a &= .2 \\
\gamma_f &= 1.0 \\
\gamma_s &= 1.2 \\
Q_s &= .0000974 \text{ ft/day} \\
\Delta x &= 231 \text{ ft}
\end{aligned} \qquad (101)$$

Following McElwee (1985) the model was set up with 79 active nodes. The river is at node 40 with a base flow from the ground-water system of $N(40) = Q_p(40) = -.154$ ft/day . Constant value boundaries are assumed for all three quantities ϕ^f, Z_b, and δ at nodes 0 and 80. The maximum saturated thickness in this area is about 40 feet.

Using this data McElwee (1985) found that unstable upconing was occurring under the river. The profile generated by McElwee using the sharp interface approximation is shown in Figure 1. In all figures only the first 40 nodes are shown; except for figures 3 and 4 all results are symmetric about the river, node 40. The interface was assumed to intercept the bottom of the river when it was 10 feet below the water table at node 40. One of the objectives of this study is to see if the dispersion of saltwater through a transition zone can significantly alter the results shown in Figure 1. In particular, is it possible for a stable upconing situation to exist if dispersion of saltwater is allowed?

PROGRAM VERIFICATION

We have written implicit, explicit and Crank-Nicolson point iterative computer programs to implement equations 12, 45 and 38 or 61. In order to check the validity of the computer programs, several tests were run. In particular, analytical results can be obtained for simple cases. The simplest test is to see if initial horizontal surfaces for ϕ^f, Z_b, and δ are maintained with no imposed stresses. Then the effects of constant areal recharge of freshwater, constant areal recharge of saltwater from below, and constant areal hydrodynamic dispersion can be tested independently. The program results checked with known analytical behavior. The transition zone and saltwater zone can be disabled in the code so only the freshwater zone is modeled. We ran a few situations to verify that the freshwater zone was being modeled correctly. The numerical programs were written separately using different numerical techniques. Therefore, a good comparison of results between them would indicate both are working correctly. This was the case for several test runs.

By setting $\delta = 0$, we have the sharp interface approximation. We attempted to reproduce the sharp interface result (McElwee, 1985) shown in Figure 1. The results were almost identical to those of McElwee. This is further evidence that the programs are working correctly. The analytical sharp interface solution given by equations 97, 99, and 100 was used as a further check on the validity of the programs developed for this study. The amount of precipitation recharged to the aquifer (N) and the amount of groundwater baseflow to the river (Q_p)are the quantities that determine whether a system will have unstable upconing, if the other physical parameters are held constant. A systematic application of equations 97, 99, and 100 shows that the Smoky Hill River system could be in a state of stable upconing if N and Q_p are about 40% of the values given earlier and $Q_s = 0$. The influx of saltwater (Q_s) from the bottom should be set to zero since for stable upconing there is no discharge of saltwater to the river; also the analytical solution assumes no saltwater flow. However, increasing Q_p and N to about 50% of their expected values gives unstable upconing again. This stable upconing of the sharp interface for 40% of N and Q_p is shown in figure 2. We are able to verify this stable interface with the programs developed for this study. The approach to steady state for stable upconing is very slow, so the explicit program is difficult to use to produce figure 2. However, if the analytical results are used as the initial conditions, the explicit program allows very little movement of these initial surfaces. If an accelerated time step is used, the implicit and Crank-Nicolson programs described earlier can be used to generate the steady state solution. However, the approach to steady state is slow and a small decaying oscillation about steady state is observed. Apparently, the two surfaces (the free surface and the saltwater interface) behave somewhat like a system of two masses tied together by a damped spring; decaying oscillations around the steady state position can be observed if the surfaces are disturbed slightly. However, the approach to steady state and the oscillations are on such a long time scale that they probably have little or no significance in a real physical system, since other shorter period and larger magnitude disturbances will be present.

The two analytical solutions for the transition zone thickness (δ) presented in equations 89 and 93 can also be used to check validity of the programs developed for this study. Consider the analytical solution given by equation 93. For this test we choose the same physical parameters as the Smoky Hill valley system (equation 101) with the following exceptions. All source and sink terms $N, Q_p,$ and Q_s are set to zero. Constant gradients for ϕ^f and Z_b are taken to be -.05/231 and 0, respectively. As constant boundary value conditions at x = 0 we choose $\phi^f(0) = 40$ ft, $\delta(0) = 1.0$ ft, and $Z_b = 1.7$ ft. In additon, α_T is needed to calculate D_T from equation 25. We choose $\alpha_T = .0015$ ft. The analytical solution is shown in figure 3 as solid curves for steady state and at a time of 5335 days. The explicit program with the Lax approximation ($\varepsilon = 0$ in equation 74) and the ideal time step of $\Delta t = \Delta x / v_h = 533.5$ days exactly reproduces the analytical solution of figure 3. However, if a smaller time step is chosen we have some numerical dispersion and the resulting solution is smoothed somewhat. This effect is seen as the dashed curve in figure 3, for a time step of 53.35 days at elapsed time of 5335 days. However, in general the numerical solution is quite adequate.

The analytical solution of equation 89 requires $\nabla\phi^f$ and ∇Z_b to be equal so we choose both to be -.05/231. Keeping the same boundary values at x = 0 for ϕ^f, Z_b, and δ as before gives the constant thickness T=38.3 ft. We may have a constant withdrawal rate, Q_p, from the freshwater-transition zone combination layer. We choose $Q_p = .56 \times 10^{-4}$ ft/day uniformly distributed over the lateral extent of the transition zone. A time step of 11.5 days is chosen for the numerical solution. All other parameters, such as $\alpha_T = .0015$ ft., remain the same as used previously. The results are shown in figure 4. The analytical solution to equation 85 is shown by the solid lines while the numerical solution by equation 74 with $\varepsilon = .9$ is given by the dashed lines. The curve shown as long dashes represents the numerical solution for 6900 days when C_2 is set to zero in equation 74. The steady-state solution for $C_2 = 0$ is within about 1% of the analytical solution and cannot be distinguished in figure 4. The third set of curves, shown with short dashes in figure 4, represent the numerical solution of equation 74 when C_2 is not equal to zero. The C_2 term is diffusive in nature making the resulting equation no longer completely hyperbolic.

The results in figure 4 show that there is some numerical dispersion for the $C_2 = 0$ case, but it is acceptable and it decreases with time. The numerical dispersion smoothes the solution somewhat and makes it lower than the analytical solution. In real world applications the C_2 term will be present; it was ignored simply to allow an analytical solution. The short dash curves in figure 4 show the complete numerical solution including the C_2 term. The C_2 term is dispersive in nature and causes a further smoothing and lowering of the analytical solution. However, the effect of the C_2 term is not major and it is expected for typical applications, such as presented here, that equation 61 will be predominantly hyperbolic with a smaller diffusive or parabolic component. In fact, it is expected that when C_2 is not zero the effects of numerical dispersion will be of lesser importance.

This section has presented some of the tests we have run to verify the programs are working correctly. There are a few things to watch out for such as the slow approach to steady state and some numerical dispersion. However, overall program performance is satisfactory. The next section applies these programs to the Smoky Hill River valley.

APPLICATION TO THE SMOKY HILL RIVER VALLEY

The average values of parameters for the Smoky Hill River valley are given in equation 101, and the model is described immediately following. One of the objectives of this study is to see if the transition zone model developed here can significantly affect the previous sharp interface results (McElwee, 1985). The new parameter introduced in this study is the dispersivity, which controls the size and shape of the transition zone. Numerous runs of the transition zone model for a range of α_T (.0015 - 1.5 ft.) have been made. The usual procedure is to start with a thin flat layer of saltwater (1.7 ft.), a thin flat transition zone (1.0 ft.), and a steady state free surface, ϕ^f, and let them all evolve to their steady state configuration.

Profiles for three values of α_T are shown in figures 5, 6, and 7. In all three figures we still have unstable upconing under the river. Additional runs for α_T = 1.5 ft. also show unstable upconing. The vertical exaggeration of figures 5, 6, and 7 might lead one to believe the Dupuit approximation of horizontal flow is inappropriate. However, there are no slopes above three degrees. Field data (Sadeghipour et. al., 1987) for this area indicates that the concentration profile for anything above α_T = .15 ft. is probably too extensive. In fact the data suggest that α_T between .015 ft. -.0015 ft. is about the right order of magnitude. The conclusion seems to be that α_T cannot be large enough to prevent unstable upconing in this area. This is a little surprising; we had originally supposed that for large enough α_T a stable upconing situation would occur. However, a more detailed analysis reveals that will never happen. If the sharp-interface approximation predicts unstable upconing, the addition of a transition zone will not prevent unstable upconing because the most that can happen is that the concentration of the saltwater zone will be lowered by dispersion of salt into the transition zone. As the concentration of the saltwater zone is lowered the unstable upconing effect becomes stronger. The most stable situation is the presence of a high-concentration high-density layer. However, lowering of the concentration of the saltwater zone is not allowed in the present model because we assume the saltwater zone to be of constant concentration. A salt-balance equation for the saltwater zone is needed in order for the concentration to change there.

The conclusion is that dispersion has an effect on the ground-water concentration profile; but, it can not be the only mechanism feeding salt water to the Smoky Hill river. A convective effect causes unstable upconing and feeds part of the saltwater to the river. Field data collected for this project suggest that the concentrations fall off away from the river much faster than shown in figure 7. Therefore, one might expect the value of α_T in this area to be considerably below .15 ft. This is in agreement with the results of the Borden site experiment (Sudicky, 1986) where the vertical dispersion was essentially diffusion controlled. Reilly and Goodman (1987) also found that the appropriate transverse dispersivity for a site at Truro, Cape Cod, Massachusetts was very small. If one is primarily interested in the concentration profile in the ground-water system, it is clear that the transition zone must be considered either by the present approximate model or a more rigorous model. However, it appears that unstable upconing is a strong effect that discharges salt water to the river also.

An interesting sidelight to this investigation is that, if the recharge to the aquifer and the river baseflow from groundwater were not so large, a stable upconing situation could occur where the saltwater is fed to the stream by dispersion through the transition zone. As determined earlier, by an application of equations 97, 99, and 100, if N and Q_p are about 40% of their normal values in the Smoky Hill valley then a stable upconing interface can occur if $Q_s = 0$, as shown in figure 2. Holding the surfaces of ϕ^f and Z_b at their values in figure 2, equation 61 can be used to look at the development of a transition zone. At the same time, equation 32 can be used to calculate the flux of salt into the base of the transition zone. Figure 8 shows the steady state transition zone that develops for $\alpha_T = .0015$ ft. The flux of salt into the transiton zone is calculated by equation 32 to be about 20% greater than that brought into the base of the saltwater zone by leakage. However, equation 32 will over-estimate the dispersive flux because it is assumed the concentration of the saltwater zone remains constant, which it will not if more salt leaves the zone by dispersion than comes in by leakage. In order to do a better job of calculating the dispersive flux a saltwater balance equation is needed for the saltwater zone. In any case, it is clear from this calculation that an α_T in the range of .0015 - .015 ft. could produce enought dispersive flux to balance the saltwater leakage observed at the base of the alluvial aquifer in the Smoky Hill River valley. In this case, the dominant mechanism feeding saltwater to the river is hydrodynamic dispersion.

SUMMARY AND CONCLUSIONS

We present a logical development of an approximate model of saltwater upconing in aquifers. The result is three nonlinear coupled equations for the freshwater zone, the saltwater zone and the transition zone. The major assumptions in this development are as follows. We assume the Dupuit-Forchheimer approximation of horizontal flow in each layer is valid. Vertical hydrodynamic dispersion into the base of the transition zone is assumed. The magnitude of this dispersion is controlled by the transverse dispersivity α_T. Once the solute is in the transition zone it is assumed to be moved by advection only. The velocity and concentration are allowed to vary in the vertical direction in the transition zone. It is assumed that they can be represented by shape functions, which are analogous to basis functions in finite element models. The concentration of the saltwater zone is assumed constant. These assumptions give a reasonably tractable model, which is considerably better than the sharp interface approximation, but is considerably simpler than a fully three-dimensional model with variable density. This approximate model should be capable of describing many real world systems where the above approximations are reasonable.

Several numerical techniques are presented to solve the approximate model equations. Explicit, implicit, and Crank-Nicolson procedures are considered. We have written programs for each of these procedures. The explicit method gives uncoupled equations which can be solved point by point for the new time level in terms of the old time level. The explicit method is simple and easy to program but has rather stringent restrictions on the time step. The implicit method gives a set of equations that are tri-tridiagonal in form. There is an algorithm available for their solution; but, it is much more difficult to program and may be subject to round-off error for large models. Since the equations are nonlinear, an iteration scheme must be used with the tri-tridiagonal algorithm to insure a correct solution is propagated through time. A good compromise may be a point iterative Crank-Nicolson procedure. In that procedure we do not have to solve a tri-tridiagonal system of equations; one iteration loop takes care of both the system of equations and the nonlinearity. In addition, round off error is not expected to be a problem. Both the implicit and Crank-Nicolson methods are expected to be stable with regard to time step size, except for very strongly nonlinear problems. Some simple analytical solutions are presented for various restricted situations. These solutions are useful for validating the numerical solution procedures. Our results have been compared to various known analytical solutions. In addition, the results for various numerical techniques have been cross checked. The conclusion is that the approximate model equations can be solved with adequate accuracy by the numerical procedures considered here.

The approximate model has been applied to the Smoky Hill River valley in Central Kansas. This is an area known to have a dense saltwater layer near the bottom of the aquifer and with a long history of natural saltwater pollution of the river. The present approximate model basically reproduces earlier sharp interface results for this area, when the transition zone is set to zero thickness. The question we seek to answer with this model is whether hydrodynamic dispersion can be the major mechanism moving saltwater to the river. We use a range of dispersivity values which should bracket the real physical values. We find that even with the largest value of dispersivity, which gives unacceptable concentration profiles, unstable upconing occurs in this area. Therefore, the conclusion is that unstable upconing is usually one of the primary mechanisms driving saltwater to the river. However we show that, if the freshwater flow to the river is only about 40 percent of its expected value, a stable upconing situation can occur where hydrodynamic dispersion into the transition zone is the primary mechanism for moving saltwater to the river. This implies that as physical conditions change along various reaches of the stream or during the year, some areas could experience unstable upconing while others could be in a situation of stable upconing. It is expected that the current approximate model could be a useful tool in evaluating the relative importance of hydrodynamic dispersion and the transition zone in various environments, not only in Kansas but in many other parts of the world.

ACKNOWLEDGEMENT

This work was supported in part by grant number 14-08-0001-G1066 from the U.S. Geological Survey. The authors also acknowledge programming support on the implicit method by Mr. Geoffrey Bohling.

REFERENCES

Bear, J., 1979, Hydraulics of ground water: McGraw-Hill, Inc., New York.

Bear, J., and A. Verruijt, 1987, Modeling groundwater flow and pollution: Reidel Publishing Co., Dordrecht, Holland, 414 p.

Bear, J., U. Shamir, A. Gamliel, and A. M. Shapiro, 1985, Motion of the seawater interface in a coastal aquifer by the method of successive steady states: Journal of Hydrology, 76: 119-132.

Essaid, H. I., 1986, A comparison of the coupled fresh water-salt water flow and the Ghyben-Herzberg sharp interface approaches to modeling of transient behavior in coastal aquifer systems: Journal of Hydrology, 86: 169-193.

Kemblowski, M., 1984, Salt-water upconing under a river - A boundary element solution: Proceedings of the 6th International Conference on Boundary Element Methods in Engineering, QE2.

Kemblowski, M., 1985, Salt-water/fresh-water transient upconing - An implicit boundary-element solution: Journal of Hydrology, 78 (1/2):

Kemblowski, M., and C. D. McElwee, 1986, Approximate model of saltwater upconing in aquifers: Kansas Geological Survey Open File Report, 86-8, 27 p.

Kemblowski, M., and J. D. Colthart, 1989, An approximate solution to the soluble plume transport near the hydrocarbon-groundwater interface: Journal of Hydrology.

Kemblowski, M., 1987, The impact of the Dupuit-Forchheimer approximation on salt-water intrusion simulation: Ground Water, 25(3): 331-336.

Liu, P. L. -F., A. H. -D Cheng, J. A. Liggett, and J. H. Lee, 1981, Boundary integral equation solution to moving interface between two fluids in porous media: Water Resources Research, 17(5): 1445-1452.

McElwee, C. D., 1985, A model study of salt-water intrusion to a river using the sharp interface approximation: Ground Water, 23(4): 465-475.

Mercer, J. W., S. P.Larson and C.R. Faust 1980, Simulation of salt-water interface motion: Ground Water, 18(4): 374-385.

Press, W. H., B. P. Flannery, S. A. Teukolsky, and W. T. Vetterling 1985, Numerical recipes: the art of scientific computing: Cambridge University Press, New York, 818 p.

Reilly, T. E. and A. S. Goodman, 1985, Quantitative analysis of saltwater-freshwater relationships in groundwater systems - a historical perspective: Journal of Hydrology, 80:125-160.

Reilly, T. E. and A. S. Goodman, 1987, Analysis of saltwater upconing beneath a pumping well: Journal of Hydrology, 89:169-204.

Rubin, H., and G. F. Pinder, 1977, Approximate analysis of upconing: Advances in Water Resources, 1 (2): 97-101.

Rubin, H., 1983, On the application of the boundary layer model for the simulation of density stratified flows in aquifer: Advances in Water Resources, 6,: 96-105.

Rubin, H., and A. Pistiner, 1986, Modelling fresh water injection into a partially saline partially fresh (PASPAF) aquifer: Journal of Hydrology, 87: 351-378.

Rubin, H., and Y. Rubin, 1986, Simulation of density stratified flows in aquifers: Advances in Water Resources, 9(1): 2-15.

Sadeghipour, J., P. A. Macfarlane, C. D. McElwee, and M. W. Kemblowski, 1987, Saltwater intrusion into alluvial aquifers; an evaluation of field methods and groundwater modeling techniques: Kansas Geological Survey Open File Report, 87-6, 208 p.

Shamir, V., and G. Dagan 1971, Motion of the seawater interface in coastal aquifers: a numerical solution: Water Resour. Res., 7(3): 644-657.

Sudicky, E. A., 1986, A natural gradient experiment on solute transport in a sandy aquifer: Spatial variability of hyraulic conductivity and its role in the dispersion process: Water Resources Research, 22(13): 2069-2082.

von Rosenberg, D. U., 1969, Methods for the numerical solution of partial differential equations: Elsevier Publishing Co., Inc., New York, p. 118.

Williams, W. E., 1980, Partial differential equations: Clarendon Press, Oxford, 357 p.

FIGURE CAPTIONS

Figure 1. Sharp interface approximation profile.

Figure 2. Stable upconing for 40% of expected average recharge and groundwater river baseflow.

Figure 3. Analytical solution (equation 93) and the numerical approximation for δ for a simple case.

Figure 4. Analytical solution (equation 89) and the numerical approximation for δ for a simple case. The effect of C_2 on the solution is also shown.

Figure 5. Transition zone approximation profile for α_T = .0015 ft.

Figure 6. Transition zone approximation profile for α_T = .015 ft.

Figure 7. Transition zone approximation profile for α_T = .15 ft.

Figure 8. Steady-state transition zone approximation profile for α_T = .0015 ft with stable upconing at 40% of the expected average recharge and groundwater river baseflow

Figure 1.

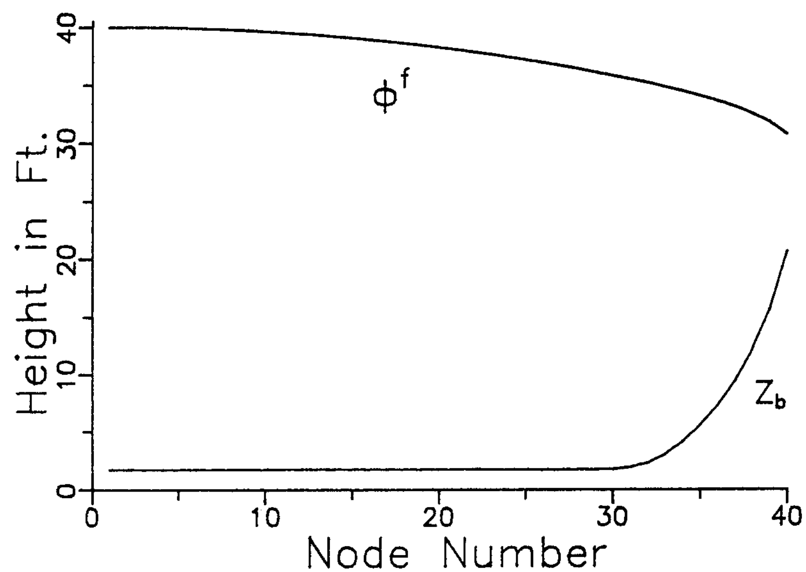

Figure 2.

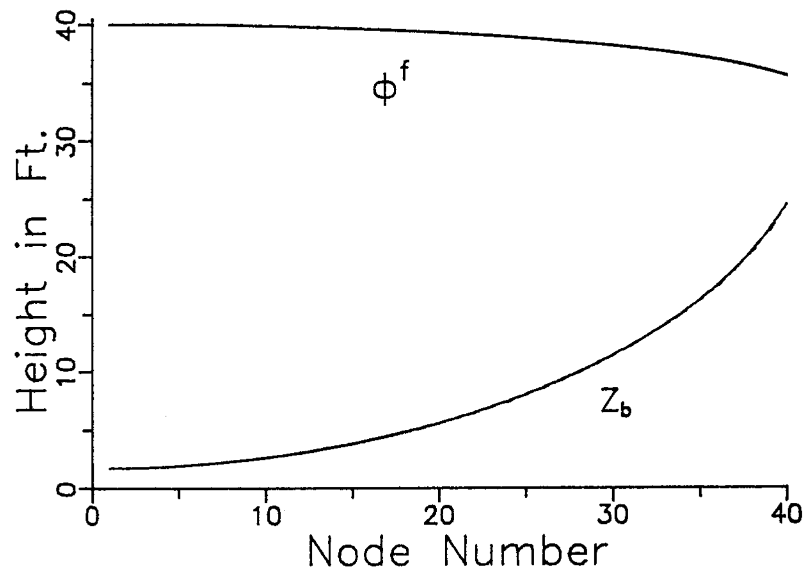

Figure 3.

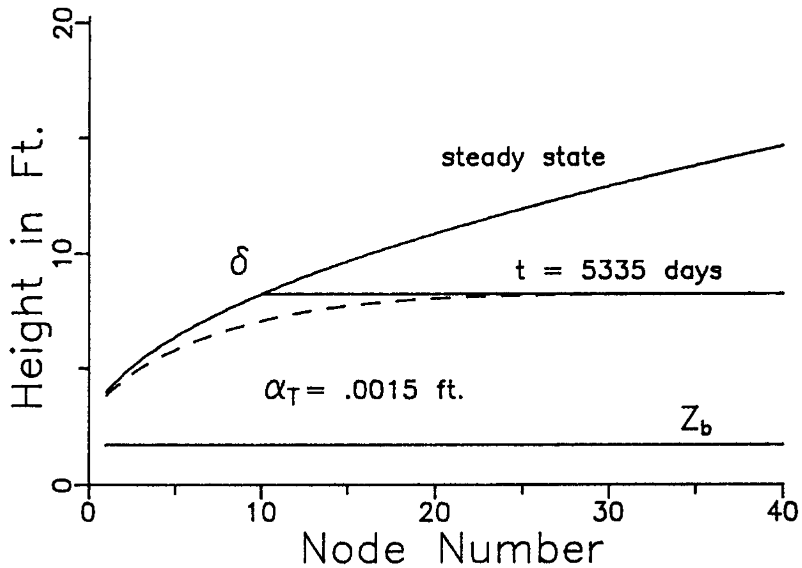

20
10
0
Height in Ft.
steady state
δ
t = 5335 days
α_T = .0015 ft.
Z_b
0
10
20
30
40
Node Number

Figure 4.

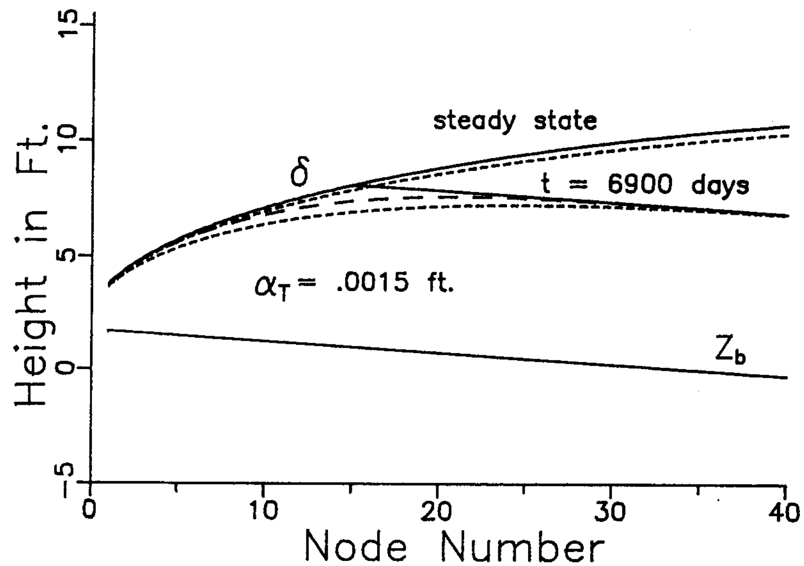

steady state
δ
t = 6900 days
α_T = .0015 ft.
Z_b
Height in Ft.
15
10
5
0
−5
0
10
20
30
40
Node Number

Figure 5.

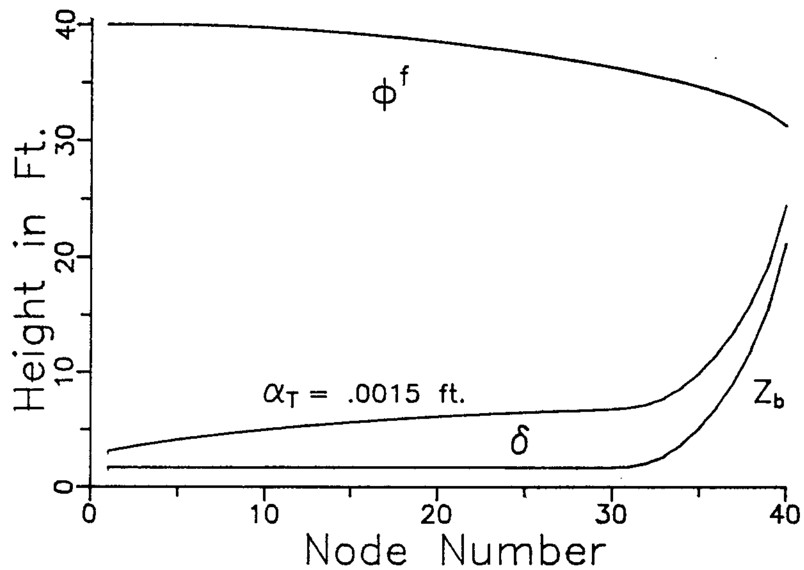
Height in Ft.
Node Number
ϕ^f
α_T = .0015 ft.
δ
Z_b
0
10
20
30
40
0
10
20
30
40

Figure 6.

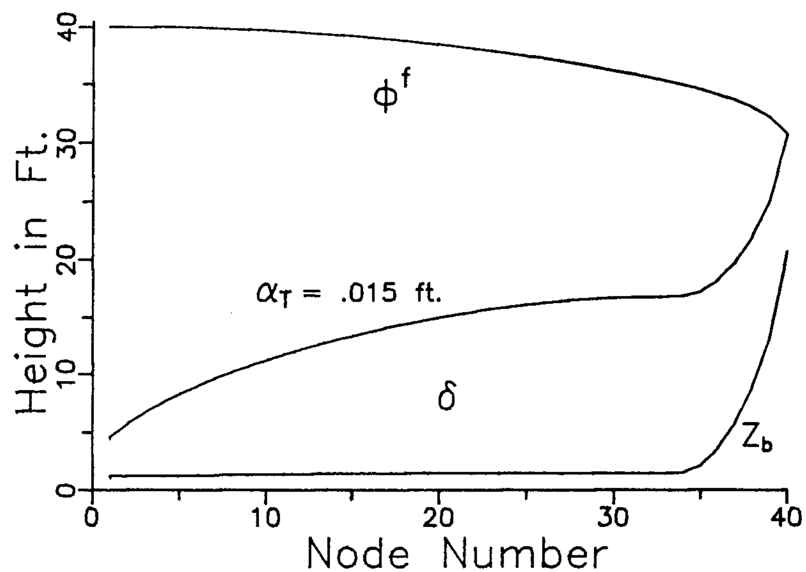
Height in Ft.
0
10
20
30
40
ϕ^f
α_T = .015 ft.
δ
Z_b
0
10
20
30
40
Node Number

Figure 7.

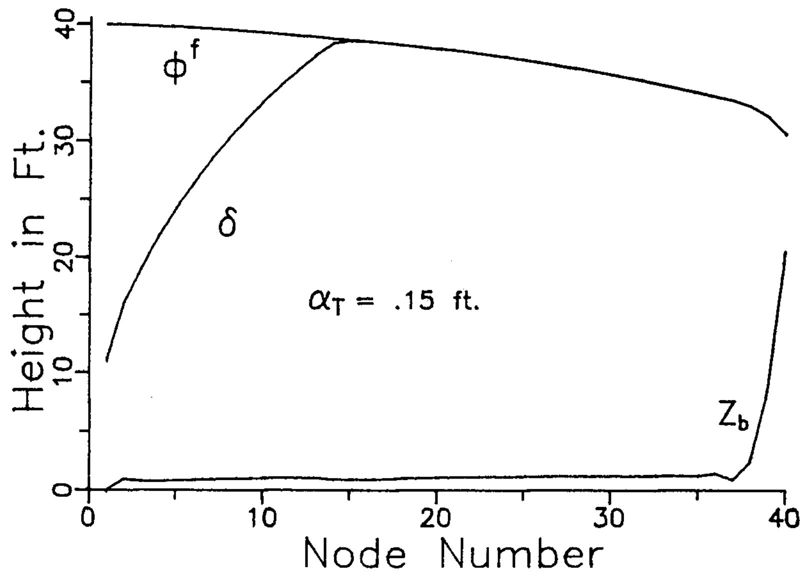

Figure 8.

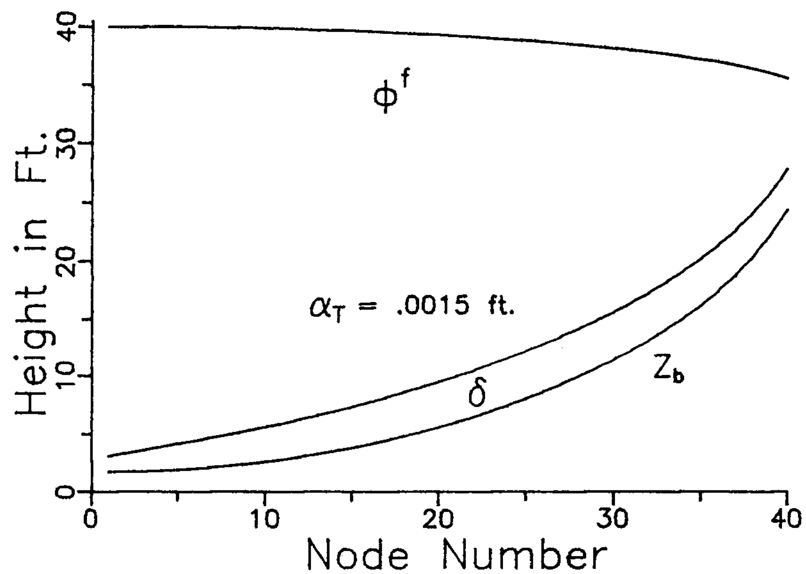

Height in Ft.
0
10
20
30
40
ϕ^f
α_T = .0015 ft.
δ
Z_b
0
10
20
30
40
Node Number